**GENERATION AND PERFORMANCE OF AUTOMATED JAROSITE MINERAL DETECTORS FOR VIS/NIR SPCTROMETERS AT MARS.** M. S. Gilmore[1], B. Bornstein[2], M. D. Merrill[1], R. Castaño[2] and J. P. Greenwood[1], [1]Dept. of Earth and Environmental Sciences, Wesleyan University, 265 Church St., Middletown, CT 06459 {mgilmore, mmerrill, jgreenwood}@wesleyan.edu, http://planetary.wesleyan.edu, [2]Jet Propulsion Laboratory, 4800 Oak Grove Drive, Pasadena, CA 91109 {ben.bornstein, rebecca.castano}@jpl.nasa.gov.

**Introduction:** Sulfate salt discoveries at the Eagle and Endurance craters in Meridiani Planum by the Mars Exploration Rover Opportunity have proven mineralogically the existence and involvement of water in Mars' past [1, 2]. Visible and near infrared spectrometers like the Mars Express OMEGA, the Mars Reconnaissance Orbiter CRISM and the 2009 Mars Science Laboratory Rover cameras are powerful tools for the identification of water-bearing salts and other high priority minerals at Mars. The increasing spectral resolution and rover mission lifetimes represented by these missions currently necessitate data compression in order to ease downlink restrictions. On board data processing techniques can be used to guide the selection, measurement and return of scientifically important data from relevant targets, thus easing bandwidth stress and increasing scientific return. We have developed an automated support vector machine (SVM) detector operating in the visible/ near-infrared (VisNIR, 300-2500 nm) spectral range trained to recognize the mineral jarosite (typically $KFe_3(SO_4)_2(OH)_6$), positively identified by the Mössbauer spectrometer at Meridiani Planum [1].

**Training Data**. Traditionally, SVM algorithms perform binary classifications of data, in this case jarosite vs. non-jarosite. The detector requires training on representative spectra from both classes. To reduce computation time, we first limit the detector input to those regions of the spectrum that contain characteristic features of jarosite. We also sought to avoid noise due to atmospheric water vapor at 1400 and 1900 nm that would be encountered during field tests. Jarosite typically has the following spectral features: a steep slope from 350-700 nm which is the edge of a charge transfer band, ferric crystal field transition bands at 430 nm and 930 nm, and bound water vibration bands ~1470, 1850, 2250 and 2500 nm [3,4] (Fig. 1). While the 430 nm band is specific to jarosite, this band is often lost in noise in our laboratory spectra and omitted in this initial test. We selected two spectral intervals over which the detector will operate: 500-1350 nm and 2050-2380 nm. Compositional variability in jarosite (natrojarosite $NaFe_3(SO_4)_2(OH)_6$, plumbojarosite $PbFe_3(SO_4)_4(OH)_{12}$, hydronium jarosite $(H_3O)Fe(SO_4)_2(OH)_6$) are found to have minimal effect on band positions [5], and thus the detector should apply to these endmembers.

Proper classification by the algorithm is facilitated by training on many representative examples. For training data, we created linear mixtures of USGS speclib 04a [6] end-member mineral spectra, using our generative model [7]. As input to the model, we included the nine jarosite spectra available in speclib 04a in one jarosite class; these spectra include jarosite (K-rich), natrojarosite and hydronium jarosite. For the non-jarosite class, we chose minerals consistent with martian petrology (basalt constituents and their weathering products) and minerals that typically occur with jarosite: alunite, anhydrite, chromite, clinochlore, epsomite, ferrihydrite, goethite, gypsum, halite, hematite, kaolinite, lepidocrosite, magnetite, montmorillonite, olivine, pigeonite, and siderite. Nontronite was omitted in this initial test due to its similarity to the jarosite spectrum in the vis/NIR. In total, we created 100 mixed spectra (50 jarosites and 50 non-jarosites). Out of 100 spectra, 25% were pure end-members, while each remaining 25% were binary, tertiary, and quaternary mixtures of end-members.

SVMs apply a kernel function to map data from its original feature space to a higher dimensional space. In the new space, data may be easier to separate into two classes. During training, examples (vectors) closest to the boundary of each class are chosen. These vectors support (define) a margin, the middle of which is the decision boundary. Later, when the SVM is presented with a new, unseen datum, the support vectors are used to determine on which side of the decision boundary the datum belongs.

The detector output is >0 (+) for a match to the jarosite class and <0 (-) for spectra with a match to the non-jarosite class.

**Detector Testing**. After training, the detector was tested on laboratory spectra of known jarosite samples from Wesleyan University's Peoples Museum. Spectra were collected with an ASD FieldSpec® FR operating over 350-2500 nm. Spectra were taken of multiple locations on each sample to include variations in crystal size and color. Additionally, 200 non-jarosite (evaporites and iron oxides) laboratory spectra of 22 pure mineral

specimens were collected and analyzed to determine the detector's ability to correctly reject samples.

To better assess the sensitivity of the jarosite detector to mineral assemblages more typical of what is seen in the field, laboratory spectra were collected of samples taken from the Sulphur Springs hydrothermal field in St. Lucia in June and November 2004, where jarosite typically occurs as a hydrothermal alteration product [8]. Finally, the detector was run on spectra of Sulphur Springs samples directly taken in the field to test the sensitivity of the detector to changing light and atmospheric conditions and consequent signal:noise. Jarosite was confirmed in a subset of the samples by X-ray Diffraction (XRD) and Scanning Electron Microscope Energy Dispersive Spectrometry (SEM-EDS), the remaining spectra were inspected and compared to published spectra [3,6,9].

**Results and Discussion**. These results pertain to the averaged spectra of 169 samples, where 10-20 spectra were averaged. The SVM jarosite detector correctly identified the presence of jarosite in the averaged spectra of 8/8 specimens and correctly rejected spectra of 22/22 museum quality samples taken under laboratory conditions. These samples are near pure jarosites and therefore most similar to the training spectra.

The detector correctly identified jarosite in the spectra of 13/16 (81%) samples of field rocks taken under laboratory conditions. The detector correctly rejected spectra of 54/56 (96%) samples where jarosite is not identified chemically or spectrally. In spectra taken in the field, the detector correctly identified jarosite in the averaged spectra of 17/20 (85%) samples and correctly rejected jarosite in 45/48 (94%) samples. Both field and laboratory spectra incorrectly classified as jarosite appear to have two of three spectral features characteristic of jarosite: a steep positive slope in the visible, a broad~900 nm absorption or a ~2200 nm absorption (Fig. 1).

These results do show the ability of the detector to recognize jarosite in natural mixtures both in the laboratory and field conditions. In these samples, jarosite is often found in intimate contact with alunite (typically $(K,Na)Al_3(SO_4)_2(OH)_6$), goethite FeO(OH) and gypsum $CaSO_4 \cdot 2H_2O$ [8] (Fig. 1). Spectra from the field samples frequently contain absorptions from two or more of these minerals. The detector is successful in distinguishing jarosite from this hydrated assemblage of sulfates and oxide.

**Conclusions.** Laboratory and field spectra of 169 samples of pure mineral and rocks samples were analyzed using the SVM jarosite detector. The detector correctly classified samples with an overall success rate of 94%. The detector performs best on pure mineral specimens but was able to distinguish jarosite in mineral assemblages typical of a hydrothermal environment. We are in the process of quantifying the percentage of jarosite required for correct identification. A detector such as this may provide a means for spectrometers to recognize jarosite at Mars autonomously.

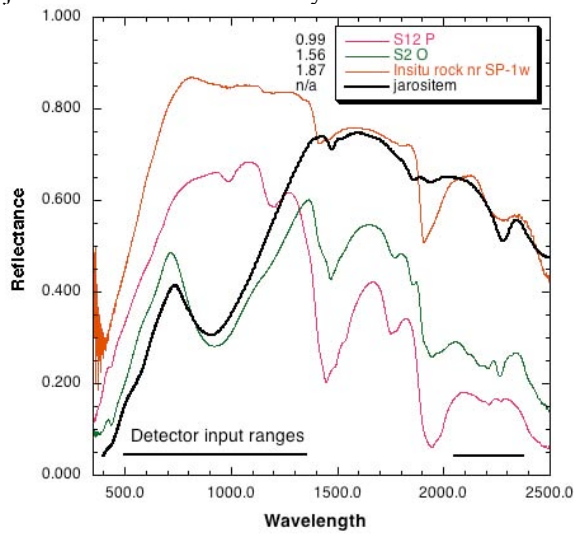


**Figure 1. Example laboratory spectra of field samples the detector identified as jarosite compared to library spectrum of jarosite (black line). Detector scores are indicated left of the key. The green spectrum contains jarosite correctly identified by the detector. The other spectra were incorrectly identified by the detector as jarosite. Those in the know will note the presence of gypsum and alunite in the spectra of the field samples.**

**References:** [1] Klingelhöfer, G. et al., 2004, *Science 306*, 1740. [2] Squyres, S.W. et al., 2004, *Science 306*, 1698. [3] Hunt et al., 1971, *Mod. Geo. 3*, 1; Hunt and Ashley, 1979, *Econ. Geo. 74*, 1613. [4] Morris et al., 1996, in: *Mineral Spectroscopy: A Tribute to Roger G. Burns*, 327. [5] Krenn et al., 2001, *LPSC XXXII*, #1223. [6] Clark, R.N., et al., 1993, *U.S.G.S. Open File Report 93-592*, 1340 pp., http://speclab.cr.usgs.gov. [7] Bornstein, B., et al., 2005, *Proc. IEEE Aerospace Conf., Big Sky, MT, IEEEAC paper #1527*, 7 pp. [8] Greenwood et al., this volume. [9] Hooke, 2000, The JPL ASTER Spectral Library v1.1, http://speclib.jpl.nasa.gov.

**Acknowledgements.** This research is supported by the NASA Applied Information Systems Research Program. XRD and SEM-EDS analyses were conducted at Yale University. Field assistance by J. Andrew Gilmore is appreciated. Special thanks to the Sulphur Springs Park in St. Lucia managed by the Soufriere Foundation.